Phase Behavior and Molecular Aggregation in Bulk Poly(2-methoxy-5-(2′-ethylhexyloxy)-1,4-phenylenevinylene)

S. H. Chen, A. C. Su,* and H. L. Chou

Institute of Materials Science and Engineering, National Sun Yat-sen University, Kaohsiung 804, Taiwan

K. Y. Peng and S. A. Chen

Department of Chemical Engineering, National Tsing Hua University, Hsinchu 300, Taiwan

Received May 26, 2003; Revised Manuscript Received October 21, 2003

ABSTRACT: Structural evolution and morphological development in films of poly(2-methoxy-5-(2′-ethylhexyloxy)-1,4-phenylenevinylene) (MEH-PPV, drop-cast from toluene solutions) upon isothermal heat treatment at elevated temperatures were studied by means of a combination of differential scanning calorimetry, polarized light microscopy, X-ray diffraction, transmission electron microscopy, ultraviolet−visible spectroscopy, and photoluminescence spectroscopy. Results indicated that MEH-PPV is mesomorphic in nature (optically biaxial, showing nematic-like texture under cross-polarization), with glass transition temperature T_g = ca. 80 °C and isotropization temperature T_i = ca. 290 °C. Upon short-term (i.e., 5 min) heat treatment at elevated temperatures (T_a) below T_i, MEH-PPV chains stack into boardlike entities (ca. 1.6 nm in thickness and ca. 0.4 nm in interbackbone spacing) within beadlike domains ca. 10−20 nm in size, which in turn aggregate transversely into wormlike features ca. 200 nm in length. Shearing at an elevated temperature results in disintegration of the wormlike agglomerates, leaving the beadlike domains arrayed into wavy lines transverse to the shear direction. Accompanying the morphological changes, ultraviolet−visible light absorption and photoexcited emission spectra vary systematically with improvement or disruption of the mesomorphic order.

Introduction

Electroluminescence (EL) properties of conjugated polymers have received widespread interests since 1990.[1] A vast amount of effort was made on modification of chemical structure for purposes of color tuning or improvement of device performance.[2] After the pioneering report[3] of dimeric photophysical phenomena in several conjugated polymers with heteroatomic backbones, morphological effects in the light-emitting behavior of a more representative conjugated polymer, poly(2-methoxy-5-(2′-ethylhexyloxy)-1,4-phenylenevinylene) (MEH-PPV), have recently attracted much attention. This polymer has been considered as amorphous, with a glass transition (T_g) in the vicinity of 65 °C.[4,5] A growing number of evidences have generally suggested the presence of a particular emission at wavelength λ_{em} = ca. 640 nm from aggregated chains in solution-cast MEH-PPV films, which competes with single-chromophore emission (λ_{em} = ca. 590 nm) and low-efficiency excimer emissions (λ_{em} = ca. 700 nm or higher).[5−12] These aggregates, already in existence in solutions above a moderate concentration threshold (on the order of 1% or less), may survive the film-forming process (typically spin-coating) and affect significantly the light emission behavior.[5,8,9] Molecular aggregation in MEH-PPV solutions has previously been rationalized in terms of solvency power,[8] but the exact photophysical nature of the particular emission from the aggregated state is still a subject of controversy.[12−14] Nevertheless, as emission from interchain species may be strongly enhanced after long-term annealing at an elevated temperature (i.e., several hours at 215 °C) *after* film formation,[7,13,14] there arises a distinct possibility for the existence of a thermodynamically favored way of molecular packing in the bulk state. This is consistent with recent observations of increased optical heterogeneity in the submicron scale and decreased hole mobility after heat treatment.[11]

In an earlier communication,[15] we have reported preliminary results that demonstrate the development of significant structural order in solution-cast MEH-PPV films upon short-term heat treatments in the temperature range 180−260 °C, with accompanying changes in optical absorption and emission behavior. Reported here are more extensive results on the phase behavior of bulk MEH-PPV in general and on the structural and morphological identification of the aggregates in particular.

Experimental Section

Poly(2-methoxy-5-(2′-ethylhexyloxy)-1,4-phenylenevinylene) (MEH-PPV, chemical structure given as an inset in Figure 2b) was synthesized via the Gilch method following in general the procedure reported by Wudl et al.[16] The weight-average molecular mass and the polydispersity were ca. 400 kDa and 4.5, respectively, as determined via size-exclusion chromatography using polystyrene standards. Polarized light microscopic (PLM) observations were made by use of a Nikon Eclipse E400-POL microscope equipped with a temperature-controlled stage. A Siemens D5000 diffractometer equipped with a copper target (Kα line, with wavelength λ = 0.154 nm), a graphite collimator, and a vacuumed high-temperature sample stage was used to obtain 1-D ("powder") X-ray diffraction (XRD) profiles under a step-scan rate of 0.05° per 2 s in the scattering angle range of 2θ = 1°−41°. Transmission electron microscopic (TEM) studies were performed using a JEOL 3010 instrument under an acceleration voltage of 200 kV, at which the combined factor of wavelength and camera length has been carefully calibrated using (111), (200), (220), and (311) reflections from vapor-deposited Al thin film. Surface topographic features were examined via secondary electron images (SEI) obtained by use of a field-emission scanning

10.1021/ma034703n CCC: $27.50 © 2004 American Chemical Society
Published on Web 12/03/2003

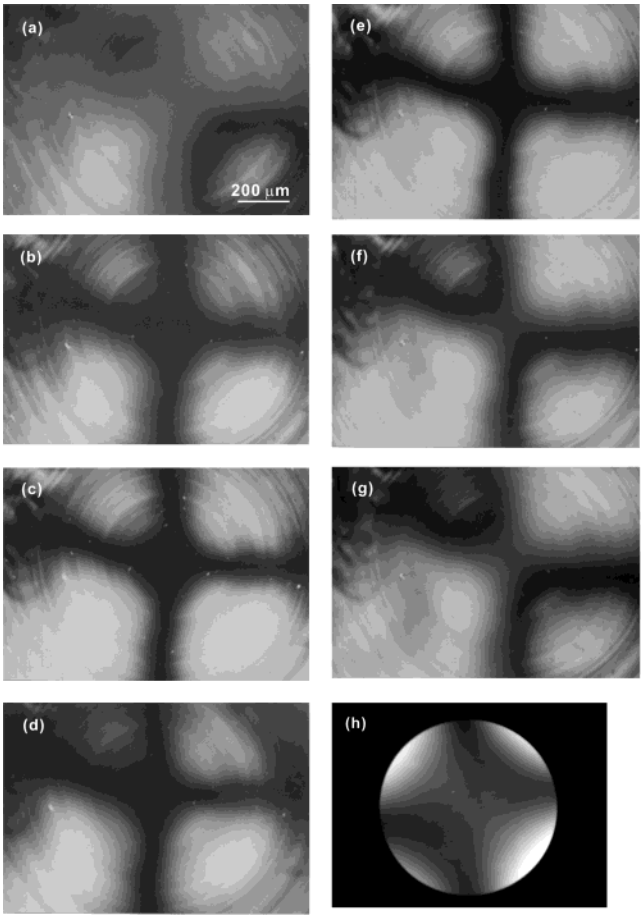

Figure 1. Polarized light micrographs of MEH-PPV film (cast from freshly prepared toluene solution) at a fixed heating/cooling rate of 20 °C/min in the temperature range of ambient to 300 °C: (a) as-cast film at room temperature, (b) heated to 60 °C, (c) 180 °C, and (d) 300 °C, followed by cooling to (e) 110 °C, (f) 60 °C, and (g) 25 °C. The conoscopic flash figure in (h) suggests optical biaxiality for specimens shear aligned at 285 °C and fast cooled to room temperature.

electron microscope (FE-SEM, JEOL JSM-6330TF) under an accelerating voltage of 10 kV. Optical absorption (UV−vis) and photoluminescence (PL) spectra of the film specimens were obtained by use of a Hong-Ming MFS-230 instrument. Fourier transform infrared spectra of heat-treated films were obtained by use of a DigiLab FTS-40 spectrometer at 2 cm^{-1} resolution.

Film specimens were drop-cast from toluene solutions (typically 0.2 wt % for PLM and XRD experiments and less than 0.1 wt % for TEM specimens) on quartz or glass substrate. Routine drying (ca. 4 h at 80 °C under vacuum) and heat treatment (5 min at an elevated temperature under a protective stream of nitrogen, followed by fast cooling to room temperature) procedures were typically adopted to follow the thermally induced structural change or its effects on absorption/emission behavior. Oriented films were obtained via manual shearing at ca. 230 °C, followed by fast cooling to room temperature. For TEM studies, specimens were detached from the substrate using aqueous HF solutions and vacuum-deposited with carbon.

Molecular simulation of MEH-PPV single chain was performed by means of the Cerius2 software on a Silicon Graphics workstation, with energy minimization achieved via iterated calculations on the basis of the Universal 1.01 all-atom force field.

Results and Discussion

Thermal Behavior. Given in Figure 1 are cross-polarized optical micrographs taken during heating and subsequent cooling of a thin, dried droplet of MEH-PPV on glass substrate. The optical texture is clearly anisotropic and nematic-like (yet lacking Schlieren features typically observable in nematic domains of such a large size), with reversible thermochromic changes (from orange-red to orange-yellow, indicating blue-shifted absorption) upon heating toward or cooling from its isotropization temperature (T_i) around 290 °C. The reversible change in the Maltese-cross pattern from room temperature to 100 °C indicates effects from thermal stresses. This implies a change in elastic modulus or the presence of a glass transition (T_g) between 60 and 100 °C. Conoscopic observations over shear-aligned specimens suggested optical biaxiality, similar to the previous report[17] on sanidic aromatic polyamides.

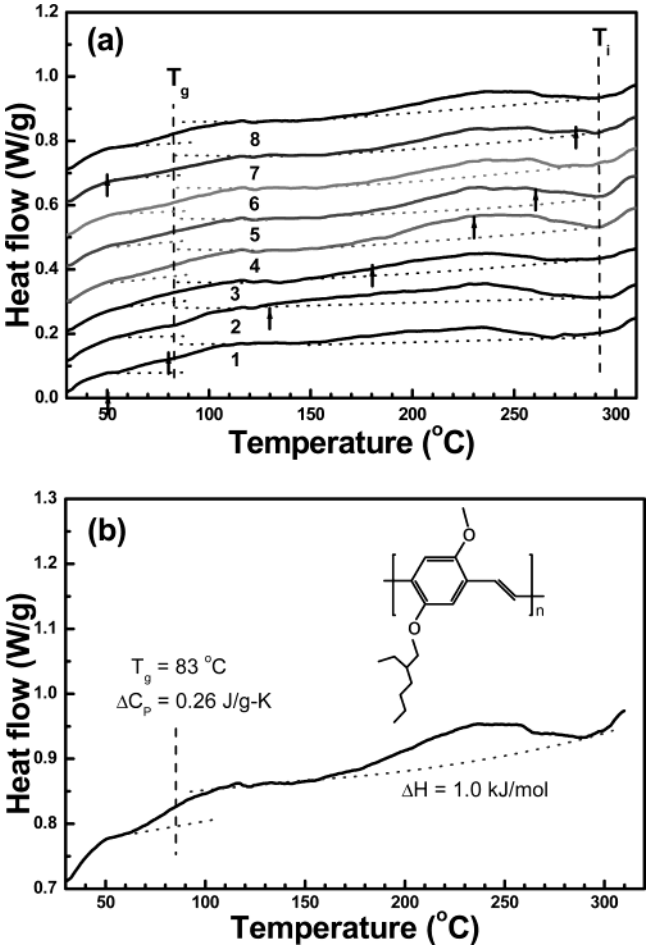

Figure 2. DSC thermograms of MEH-PPV at a heating rate of 20 °C/min after annealing and fast cooling to and equilibration at 10 °C. Traces in (a) correspond to heat treatment conditions of (1) 50 °C for 30 min, (2) 80 °C for 30 min, (3) 130 °C for 30 min, (4) 180 °C for 30 min, (5) 230 °C for 10 min, (6) 260 °C for 10 min, (7) 280 °C for 5 min, and (8) 50 °C for 12 h. Arrows indicate the temperature of isothermal annealing. An expanded view of curve 8 in (a) is shown in (b).

Shown in Figure 2 are a series of DSC reheating thermograms obtained after fast cooling from elevated temperatures (ranging from 50 to 280 °C) at which the specimen had been isothermally annealed for various periods (10 min to 12 h) of time. Consistent with the PLM observations, there is a glass transition at ca. 80 °C which is slightly higher than that (ca. 70 °C) estimated via a group-contribution method.[18] The average heat capacity jump across T_g is $\Delta C_p = 0.27$ J g^{-1} K^{-1}, yielding $T_g \Delta C_p = 95$ J/g, which is in fair agreement with the empirical Simha−Boyer rule.[19,20] There is also

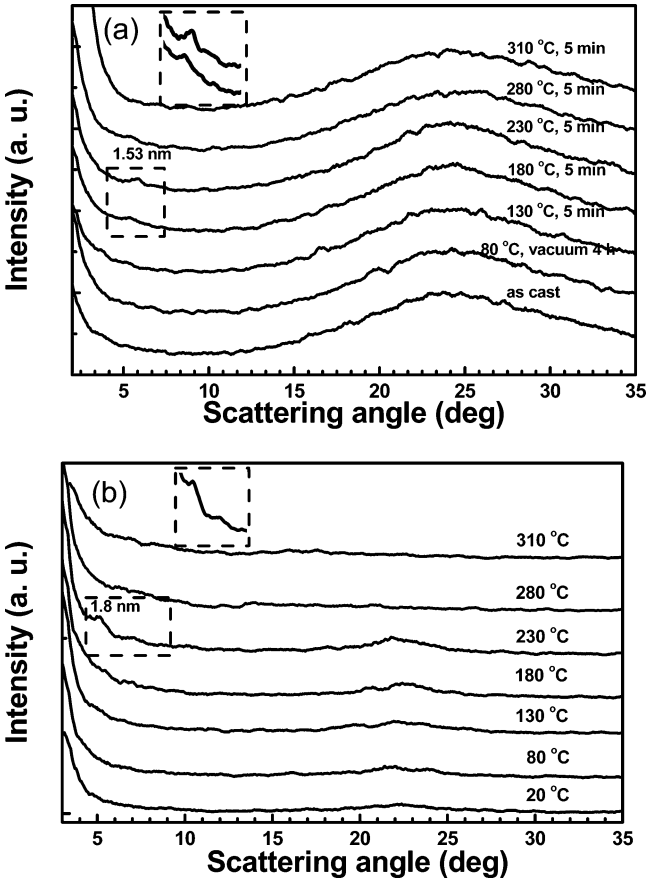

Figure 3. (a) Room temperature XRD profiles of MEH-PPV film upon fast cooling to room temperature during a sequence of 5 min heat treatments at stepwise increased T_a. (b) High-temperature XRD profiles of MEH-PPV film during stepwise increases in temperature. The films were cast from freshly prepared toluene solution.

a broad and weak endotherm spanning the temperature range 150−290 °C, which is insensitive to heat treatment; the average value for the heat of transition is ΔH_i = ca. 1.1 kJ/mol, much smaller than typical values for a crystalline phase but close to those in the nematic-to-isotropic transition of liquid crystals. This low value of heat of transformation and the lack of clear changes in thermal behavior with heat treatments at elevated temperatures imply that the transformation is thermally weak, involving mainly secondary intermolecular interactions, much like microphase separation in block copolymers.

Structural Development upon Heat Treatment. Given in Figure 3a are room temperature XRD powder profiles of MEH-PPV film fast-cooled from the 5 min isothermal annealing at increasingly higher heat treatment temperatures (T_a). The XRD profiles remain featureless for $T_a \leq 130$ °C, which explains for the earlier belief of MEH-PPV being amorphous. At T_a = 180 °C, a peak emerges in the vicinity of $2\theta = 6°$ with a d spacing value of ca. 1.5 nm which becomes better developed at 230 °C, indicating some form of long-range nanoscale modulation. This peak dissipates at $T_a > 280$ °C, consistent with PLM and DSC observation. The formation and the dissipation of an ordered phase in the temperature range 200−300 °C is confirmed via high-temperature XRD profiles obtained at stepwise increased temperatures (cf. Figure 3b). Note that, in the high-temperature XRD profile obtained at 230 °C, the peak corresponding to the nanoscale modulation corresponds to a d spacing value of ca. 1.8 nm. This translates to a thermal expansion coefficient of ca. 800 ppm/K, revealing some liquidlike characteristics. We note that the corresponding peak in the XRD profile reported in our earlier communication (as Figure 2 therein)[15] was stronger and more easily identifiable. The difference is that, in the earlier case, the toluene solution used for film-casting was "aged" for 16 days after solution preparation. This "storage effect" effect is indeed significant and will be the subject of future reports based on small-angle X-ray and neutron scattering measurements over MEH-PPV/toluene solutions[21] as well as TEM observations over MEH-PPV films cast from toluene solutions.[22]

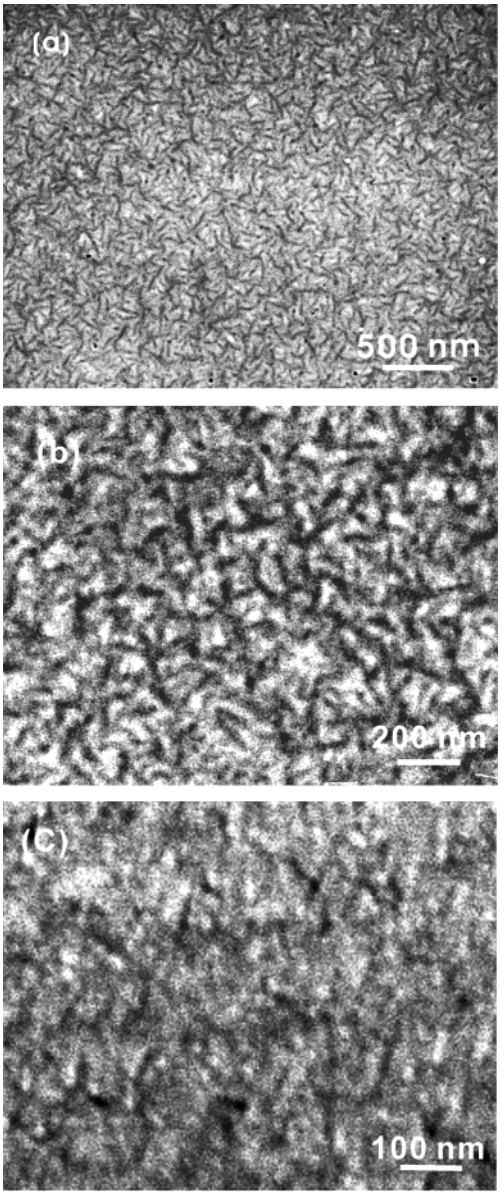

Figure 4. (a) Representative TEM bright field image of annealed specimens (5 min at 230 °C, followed by fast cooling to room temperature), (b) expanded view, and (c) field-emission SEM micrograph (secondary electron image) showing more clearly the beadlike feature (bright dots) of the nanograins as well as cracks (wiggling dark lines) formed under electron beam suggest poor intergrain cohesion. Specimens were cast from freshly prepared toluene solution.

Shown in Figures 4 and 5 are TEM bright-field images obtained from annealed (5 min at 230 °C, followed by fast cooling to room temperature) and

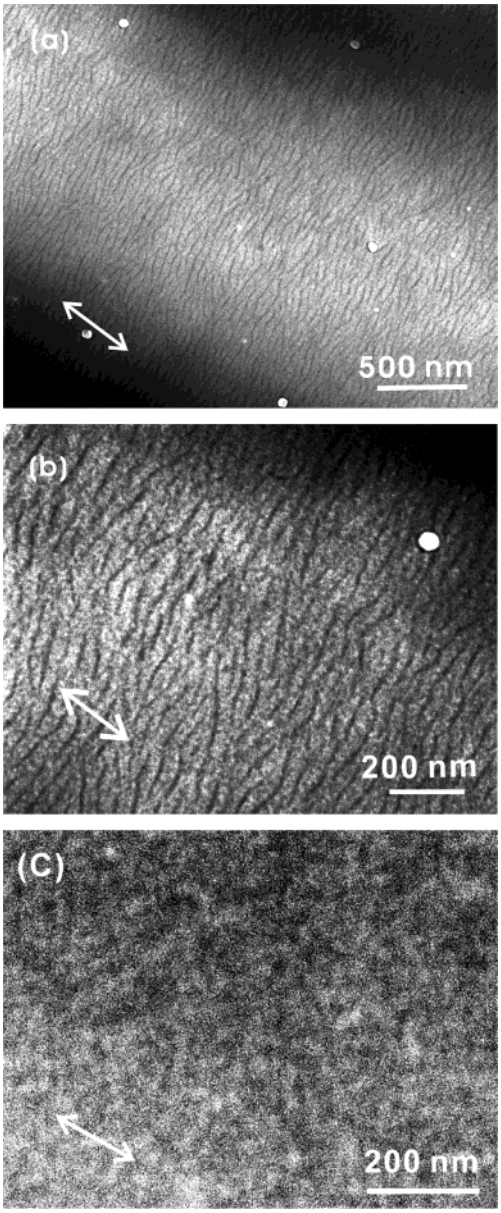

Figure 5. (a) TEM bright field images of specimens manually sheared at the end of the 5 min annealing at 230 °C before fast cooling to room temperature; (b) expanded view. (c) FE-SEM micrograph (secondary electron image) showing the beadlike feature (bright dots) of the nanograins. Two-way arrows indicate the direction of shear. Specimens were cast from freshly prepared toluene solution.

sheared (right after the 5 min annealing at 230 °C, followed by fast cooling to room temperature) specimens. The annealed specimens are characterized by the presence of wormlike entities (of higher electron density as determined via an over- and underfocusing procedure) approximately 10−20 nm in width and 200 nm in length (cf. Figure 4a). The expanded view (cf. Figure 4b) indicates that these "worms" are in fact composed of a string of beads ca. 10−20 nm in size, as also observed via FE-SEM (SEI, cf. Figure 4c). The action of shear resulted in the disintegration of "worms" and the rearrangement of constituting beads into wavy arrays transverse to the direction of shear as shown in Figure 5a. [We emphasize here again that these features were due to contrast in electron density, and the shear action was made in the melt state; these are not to be confused with the flow-induced band features[23] in films cast from a lyotropic liquid crystalline phase via a particular film formation scheme (i.e., on a slightly tilted substrate with slow evaporation of solvent under a saturated atmosphere) as there are orders-of-magnitude differences in the length scale.] These beads are again more easily identifiable in the expanded view (cf. Figure 5b) and in the corresponding SEI (cf. Figure 5c) obtained via FE-SEM.

Selected-area diffraction (SAED) patterns obtained over shear-aligned specimens are characterized by (1) equatorial reflections with *d* spacing values of 1.60 and 0.40 nm and (2) meridional reflections with *d* spacing values of 0.67, 0.34, and 0.22 nm. Error bounds of these data are typically within 3%. (Note that the values given in our earlier communication[15] are erroneous due to inadequate calibration. The interpretations given therein are therefore incorrect; our revised view is given as the following.) The structure is therefore consistent with the sanidic picture proposed previously by Watanabe et al.[24] for aromatic polyesters with flexible side chain, in which the rigid backbone aggregated to give boardlike characteristics whereas the side chains extend more or less along the plane normal, rendering the "boards" approximately equal-spaced. In the present case of MEH-PPV, the "boards" are only imperfectly arrayed with a distribution of interboard centered around 1.6 nm, in view of the absence of the higher-order reflections. The equatorial reflection ca. 0.4 nm in *d* spacing cannot be attributed to the fourth-order reflection of the lamellar arrangement due to the absence of the second- and third reflections; instead, it is taken as the in-plane spacing between backbones. The meridional arcs correspond to monomeric repeats ca. 0.67 nm along the backbone; this is consistent with previously reported value of 0.67 nm for PPV[25−28] and 0.65 nm for MEH-PPV[29] on the basis of X-ray diffraction results. Our molecular mechanics calculations over MEH-PPV single chains of various possible configurations (i.e., head-to-tail, head-to-head, and their randomized hybrid) indicated a value of 0.66 nm for the monomeric repeat length. Note that the horizontal streaking of the first meridional arc implies the presence of stacking faults parallel to the mean backbone axis.[30]

In this picture, the in-plane backbones are aligned to give nematic-like texture under cross-polarized light and the three principal directions (along the backbone, in-plane but transverse to backbone, and plane normal) have different refractive indices, which is consistent with the observed biaxial optical behavior. We emphasize here that the observed ordering is mesomorphic in nature. This is not to be confused with the previously proposed[29] crystalline order (orthorhombic, with lattice parameters $a = 0.712$ nm, $b = 1.605$ nm, and $c = 0.647$ nm, which is incommensurate with the present diffraction patterns) for a highly stretched (with a draw ratio of 5) MEH-PPV film, in which the backbone is fully extended in all-trans conformation along the *c*-axis. For unstretched films, a single reflection corresponding to a *d* spacing value of 1.8 nm was observed but not commented upon in terms of specific structural features.[29] We believe that this unidentified morphology is in better correspondence with the primitively layered structure reported here. Similar observations of molecular assemblies of layered morphology have been reported[31] for thin films of poly(*p*-phenyleneethynylene)s.

Morphological Model. Given in Figure 7 is a schematic model for the connection of the boardlike

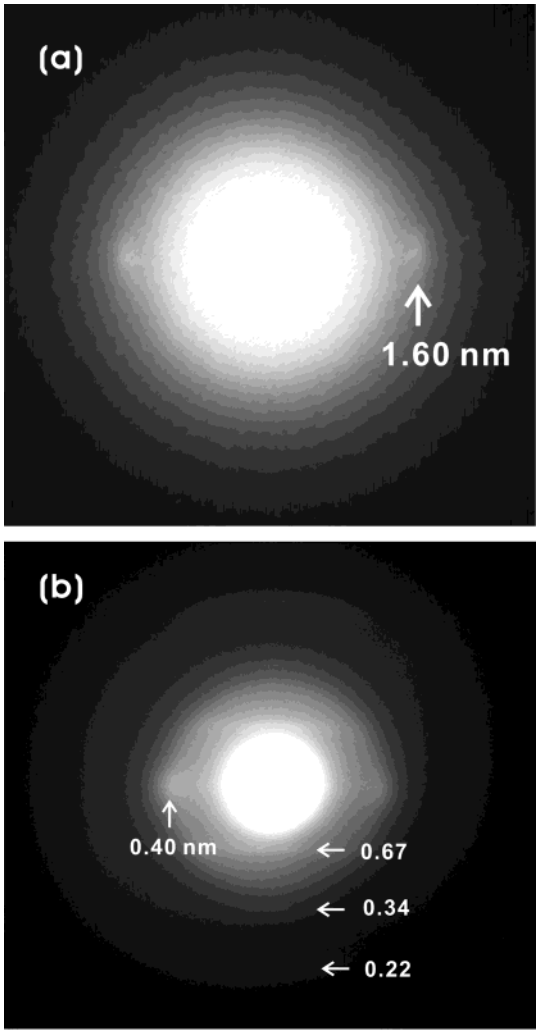

Figure 6. SAED patterns of shear-oriented specimens (cf. Figure 5, with the shear direction parallel to the meridian) showing (a) equatorial reflection corresponding to layer spacing of 1.6 nm and (b) equatorial reflection of the in-plane interbackbone spacing of 0.4 nm and meridional reflections corresponding to monomeric repeats of ca. 0.67 nm in the direction of shear.

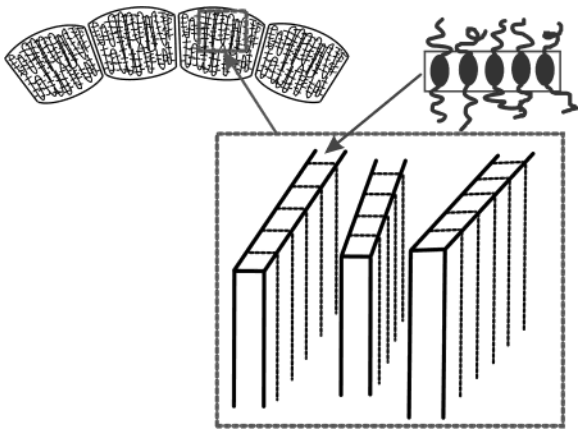

Figure 7. Schematic presentation of hierarchical features of MEH-PPV aggregates.

structure in the molecular level to agglomerated wormlike morphology observed in the electron micrographs shown in Figures 4 and 5. In the model, each bead (approximately 10−20 nm in size, with truncated flat ends) is composed of boardlike entities formed by aggregated MEH-PPV backbones. The beads, in turn, are weakly attached side by side in the transverse direction to give wormlike features. It follows that, upon shear at an elevated temperature, the "worms" are disintegrated into units of beads, within which the MEH-PPV backbones and the boardlike assemblies are aligned in the shear direction.

Similar morphological features have been observed for quite a number of hairy-rod polymers studied in this laboratory; these will be presented and discussed in detail in future occasions. Nevertheless, to satisfy curious readers, a preliminary interpretation is given as the following. In view of the small size involved, each "bead" or "nanograin" observed here must be composed of essentially single (or few) MEH-PPV chains, indicating general lack of interchain entanglements during its formation. This is most likely related to collapse of the isolated semirigid MEH-PPV chains upon increase in polymer concentration (yet still below the overlap threshold) due to the rigid-rod nature (the persistent length of MEH-PPV chains in dilute toluene solutions, as determined recently[32] via small-angle neutron scattering, is 13.5 nm, which translates to ca. 20 repeat units), which encourages phase separation at a very low concentration according to the classical nematic polymer solution theory[33] of Flory. One may imagine that the relative attraction among alkyl side chains in the presence of toluene, a not-so-favorable aromatic solvent, may contribute further to the segregation effect. More recent studies on conformation of collapsed semirigid chains in general[34] or MEH-PPV with tetrahedral defects in particular[35] have indicated a variety of possible morphological features ranging from toroids, bundles, to defective bundles. We consider these latter features highly relevant to the nanograin morphology observed here.

Optical Absorption/Emission. As shown in Figure 8, both absorption and emission spectra are significantly affected by development of the mesomorphic order upon heat treatment. The absorption edge, initially located at ca. 590 nm in the as-cast state, red-shifted to ca. 600 nm upon short-term annealing at $T_a \leq 130$ °C, red-shifted further to ca. 610 nm for $T_a \geq 180$ °C, followed by blue shift to ca. 580 nm after heat treatment at $T_a = 310$ °C. In contrast, there were a main emission at 590 nm and a secondary maximum at ca. 640 nm in the emission spectrum (excited at 480 nm) of the as-cast MEH-PPV film. The relative weighting of the 590 nm emission decreases gradually upon short-term annealing at $T_a \leq 130$ °C; for $T_a \geq 180$ °C, the 640 nm emission became dominant. The trend was reversed for $T_a = 280$ °C (which approaches T_i = ca. 290 °C); upon heat treatment above T_i (i.e., at the highest T_a of 310 °C), the short-wavelength emission at ca. 590 nm became the dominant emission again. These changes correspond fairly well to the emergence and the dissipation of structural order in the parallel XRD study shown in Figure 3a. The effects are more clearly demonstrated in Figure 8c, where the excitation wavelength was selected to be 590 nm. The emission at 640 nm was present even for the as-cast film (with absorption edge located near 590 nm); its intensity increased with T_a up to 130 °C, followed by a slight decrease (as emissions above 700 nm intensified), reaching the maximum at $T_a = 230$ °C. For $T_a = 280$ °C, the 640 nm emission became weakened (whereas emission intensities above 700 nm remained unchanged). After short-term annealing at $T_a = 310$ °C, all emissions, including those above

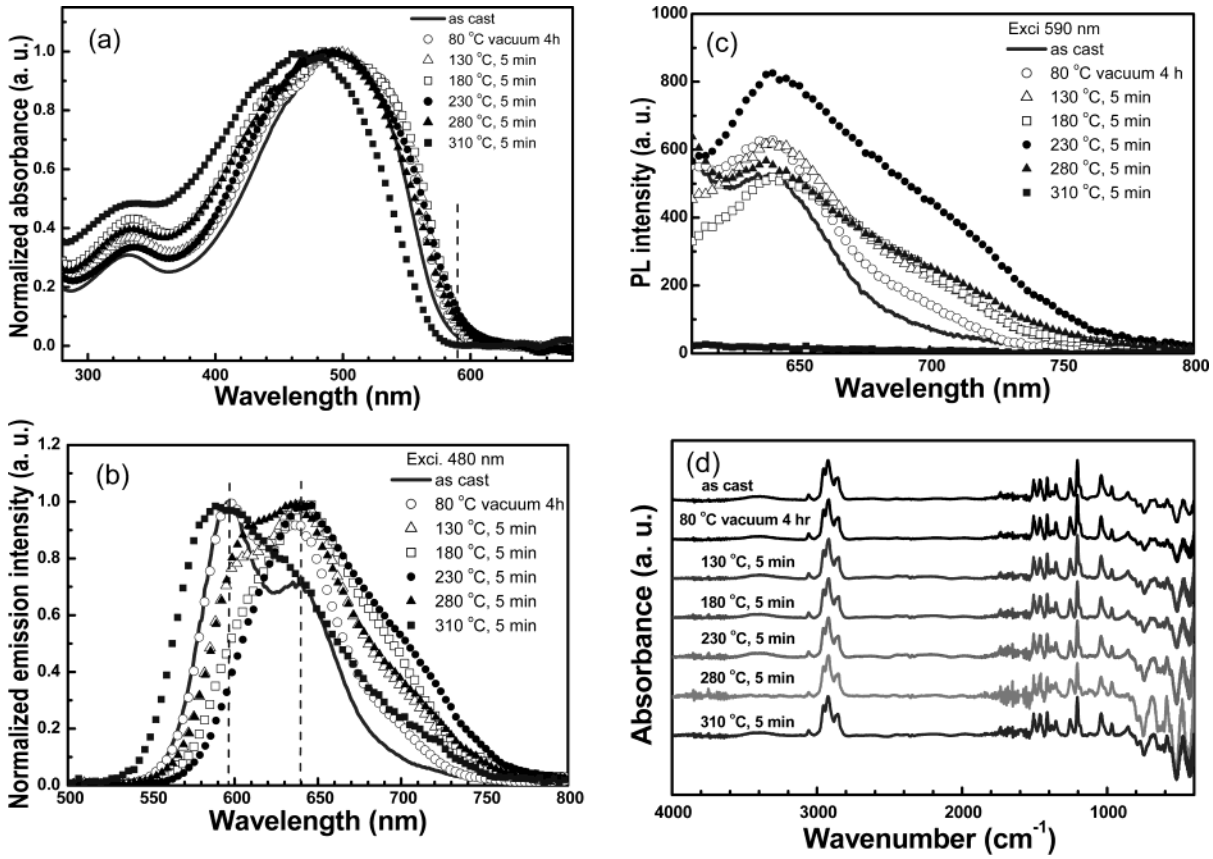

Figure 8. Normalized (a) absorption and (b) emission (excited at 480 nm) spectra of solution-cast MEH-PPV film upon fast cooling to room temperature during a sequence of 5 min heat treatments at stepwise increased T_a; (c) emission spectra upon excitation at 590 nm (i.e., near the absorption edge); (d) corresponding FTIR spectra. Note that the thermal history exactly parallels that of the XRD study in Figure 3a.

700 nm, became negligible as the excitation wavelength became longer than the absorption edge. It should be noted that all these observations are reversible upon swelling of the MEH-PPV film and not attributable to chemical degradation of the MEH-PPV film, as parallel infrared spectra (cf. Figure 7d) showed no indications of photo- or thermooxidation.

It is generally agreed that emissions at 700 nm or above are attributable to excimer emissions and the emission at 590 nm is due to single-chromophore emission. One is therefore tempted to attribute the emission to "aggregate emission" (which corresponds to physical dimers that exist not only in the excited state but also remain attached in the ground state)[36] as there is an increase in lifetime and an decrease in PL quantum efficiency.[6−8,10] On the other hand, as the two peaks differ by 1300 cm^{-1} that coincides with the vibrational frequency of the phenylenevinylene moiety, the changes in relative intensities of the two peaks may also be simply attributed to a change in the vibronic characteristics (i.e., an increase in the Huang−Rhys factor)[36] due to increased conjugation length upon aggregation. Further complications arise as recent solvatochromic results of Schaller et al.[14] indicated excimer-like nature of the 640 nm and the 700 nm emissions. However, as the energy difference between these two peaks is also approximately 1300 cm^{-1}, it is conceivable that the emission peak at 640 nm may bear some excimer-like characteristics due to contributions from the 700 nm peak via phonon coupling. Our current results clearly indicate that both the 640 nm and the 700 nm emissions are closely related to aggregation of MEH-PPV chains. It is likely that both single-chromophore excitons and excimers contribute at least partly to the emission at 640 nm via phonon coupling. Whether or not a separate mechanism of "aggregate emission" contributes significantly to the emission at this particular wavelength is beyond the scope of the present work and awaits further studies.

Conclusion

By means of heat treatment, we have demonstrate thermodynamic preference for the molecular aggregation of MEH-PPV in the bulk state, which results in a hierarchy of morphological features and bears strong effects on the light emission behavior. A model is proposed for the aggregates and the hierarchical morphological features hence developed.

Acknowledgment. This work is financially supported by the Ministry of Education and the National Science Council under Contracts 91E-FA04-2-4A and NSC91-2216-E-110-007. Thanks are due to Mr. S. R. Han and Ms. C.J. Hsu for their assistance in experimental work.

References and Notes

(1) Kraft, A.; Grimsdale, A. C.; Holmes, A. B. *Angew. Chem., Int. Ed.* **1998**, *37*, 402.
(2) Friends, R. H.; Gymer, R. W.; Holmes, A. B.; Burroughes, J. H.; Marks, R. N.; Taliani, C.; Bradley, D. D. C.; dos Santos, D. A.; Gredas, J. L.; Loglund, M.; Salaneck, W. R. *Nature (London)* **1999**, *397*, 121.
(3) Jenekhe, S. A.; Osaheni, J. A. *Science* **1994**, *265*, 765.
(4) Liu, Y.; Liu, M. S.; Li, X. C.; Jen, A. K. Y. *Chem. Mater.* **1998**, *10*, 3301.
(5) Lee, T. W.; Park, O. O. *Adv. Mater.* **2000**, *12*, 801.

(6) Nguyen, T. Q.; Doan, V.; Schwartz, B. J. *J. Chem. Phys.* **1999**, *110*, 4068.
(7) Nguyen, T. Q.; Martini, I. B.; Liu, J.; Schwartz, B. J. *J. Phys. Chem. B* **2000**, *104*, 237.
(8) Shi, Y,; Liu, J.; Yang, Y. *J. Appl. Phys.* **2000**, *87*, 4254.
(9) Liu, J.; Shi, Y.; Ma, L.; Yang, Y. *J. Appl. Phys.* **2000**, *88*, 605.
(10) Nguyen, T. Q.; Schwartz, B. J.; Schaller, R. D.; Johnson, J. C.; Lee, L. F.; Haber, L. H.; Saykally, R. J. *J. Phys. Chem. B* **2001**, *105*, 5153.
(11) Tan, C. T.; Inigo, A. R.; Fann, W. S.; Wei, P. K.; Peng, G. Y.; Chen, S. A. *Org. Electron.* **2002**, *3*, 81.
(12) Collison, C. J.; Rothberg, L. J.; Treemaneekarn, V.; Li, Y. *Macromolecules* **2001**, *34*, 2346.
(13) Schaller, R. D.; Snee, P. T.; Johnson, J. C.; Lee, L. F.; Wilson, K. R.; Haber, L. H.; Saykally, R. J.; Nguyen, T.-Q.; Schwartz, B. J. *J. Chem. Phys.* **2002**, *117*, 6688.
(14) Schaller, R. D.; Lee, L. F.; Johnson, J. C.; Haber, L. H.; Saykally, R. J.; Vieceli, J.; Benjamin, I.; Nguyen, T.-Q.; Schwartz, B. J. *J. Phys. Chem. B* **2002**, *106*, 9496.
(15) Chen, S.-H.; Su, A.-C.; Huang, Y.-F.; Su, C.-H.; Peng, G.-Y.; Chen, S.-A. *Macromolecules* **2002**, *35*, 4229.
(16) Wudl, F. US Pat. No. 5189136, 1990; *Chem. Abstr.* **1993**, *118*, 255575p.
(17) Ebert, M.; Herrmann-Schonherr, O.; Wendorff, J. H.; Ringsdorf, H.; Tschirner, P. *Makromol. Chem., Rapid Commun.* **1988**, *9*, 445.
(18) Van Krevelen, D. W. *Properties of Polymers*, 3rd ed.; Elsevier: Amsterdam, 1997.
(19) Simha, R.; Boyer, R. F. *J. Chem. Phys.* **1962**, *37*, 1003.
(20) Boyer, R. F. *J. Macromol. Sci., Phys.* **1973**, *7*, 487.
(21) Chen, H. L.; et al. Manuscript in preparation.
(22) Chen, S. H.; Su, A. C.; Chang, C. S.; Chen, H. L.; Peng, K. Y.; Chen, S. A. Submitted to *Macromolecules*.
(23) Wang, W.; Lieser, G.; Wegner, G. *Makromol. Chem.* **1993**, *194*, 1289.
(24) Watanabe, J.; Harkness, B. R.; Sone, M.; Ichimura, H. *Macromolecules* **1994**, *27*, 507.
(25) Granier, T.; Thomas, E. L.; Gagnon, D. R.; Karasz, F. E.; Lenz, R. W. *J. Polym. Sci., Polym. Phys.* **1986**, *24*, 2793.
(26) Chen, D.; Winokour, M. J.; Masse, M. A.; Karasz, F. E. *Polymer* **1992**, *33*, 3116.
(27) Zhang, X. B.; Van Tendeloo, G.; Van Landuyt, J.; Van Dijck, D.; Briers, J.; Bao, Y.; Geise, H. J. *Macromolecules* **1996**, *29*, 1554.
(28) Shah, H. V.; Scheinbeim, J. I.; Arbuckle, G. A. *J. Polym. Sci., Polym. Phys.* **1999**, *37*, 605.
(29) Yang, C. Y.; Hide, F.; Diaz-Garcia, M. A.; Heeger, A. J.; Cao, Y. *Polymer* **1998**, *39*, 2299.
(30) Tosaka, M.; Hamada, N.; Tsuji, M.; Kohjiya, S.; Ogawa, T.; Isoda, S.; Kobayashi, T. *Macromolecules* **1997**, *30*, 4132.
(31) Perahia, D.; Traiphol, R.; Bunz, U. H. F. *Macromolecules* **2001**, *34*, 151.
(32) Ou-Yang, W. C.; Chang, C. S.; Chen, H. L.; Ho, D. L.; Tsao, C. S.; Yang, G.; Peng, K. Y.; Chen, S. A.; Han, C. C. Manuscript in preparation.
(33) Flory, P. J. *Proc. R. Soc. London* **1956**, *A234*, 73.
(34) Noguchi, H.; Yoshikawa, K. *J. Chem. Phys.* **1998**, *109*, 5070.
(35) Hu, D.; Yu, J.; Wong, K.; Bagchi, B.; Rossky, P. J.; Barbara, P. F. *Nature (London)* **2000**, *405*, 1030.
(36) Pope, M.; Swenberg, C. E. *Electronic Processes in Organic Crystals and Polymers*, 2nd ed.; Oxford University Press: Oxford, 1999.

MA034703N